Available online at www.sciencedirect.com
SCIENCE DIRECT®
Journal of Nuclear Materials 341 (2005) 62–82
journal of nuclear materials
www.elsevier.com/locate/jnucmat

Effect of external gamma irradiation on dissolution of the spent UO_2 fuel matrix

C. Jégou [a,*], B. Muzeau [a], V. Broudic [a], S. Peuget [a], A. Poulesquen [a], D. Roudil [a], C. Corbel [b]

[a] Commissariat à l' Énergie Atomique (CEA), Rhône Valley Research Center, DTCD/SECM/LMPA, BP 17171, 30207 Bagnols-sur-Cèze cedex, France
[b] Commissariat à l'Énergie Atomique (CEA), Saclay Research Center, DRECAM/LSI, 91191 Gif-sur-Yvette Cedex, France

Received 24 October 2003; accepted 15 January 2005

Abstract

Leaching experiments were performed on UO_2 pellets doped with alpha-emitters ($^{238/239}Pu$) and on spent fuel, in the presence of an external gamma irradiation source ($A^{60}Co = 260$ Ci, $\dot{D}\gamma = 650$ Gy h^{-1}). The effects of α, β, γ radiation, the fuel chemistry and the nature of the cover gas (aerated or Ar + 4%H_2) on water radiolysis and on oxidizing dissolution of the UO_2 matrix are quantified and discussed. For the doped UO_2 pellets, the nature of the cover gas clearly has a major role in the effect of gamma radiolysis. The uranium dissolution rate in an aerated medium is 83 mg m^{-2} d^{-1} compared with only 6 mg m^{-2} d^{-1} in Ar + 4%H_2. The rate drop is accompanied by a reduction of about four orders of magnitude in the hydrogen peroxide concentrations in the homogeneous solution. The uranium dissolution rates also underestimate the matrix alteration rate because of major precipitation phenomena at the UO_2 pellet surface. The presence of studtite in particular was demonstrated in aerated media; this is consistent with the measured H_2O_2 concentrations (1.2×10^{-4} mol L^{-1}). For spent fuel, the presence of fission products (Cs and Sr), matrix alteration tracers, allowed us to determine the alteration rates under external gamma irradiation. The fission product release rates were higher by a factor of 5–10 than those of the actinides (80–90% of the actinides precipitated on the surface of the fragments) and also depended to a large extent on the nature of the cover gas. No significant effect of the fuel chemistry compared with UO_2 was observed on uranium dissolution and H_2O_2 production in the presence of the ^{60}Co source in aerated conditions. Conversely, in Ar + 4%H_2 the fuel self-irradiation field cannot be disregarded since the H_2O_2 concentrations drop by only three orders of magnitude compared with UO_2.

1. Introduction

The option of direct disposal of spent nuclear fuel in a deep geological formation raises the need to investigate the long-term behavior of the UO_2 matrix in aqueous media subjected to α, β, γ radiation. The release of radionuclides from the fuel matrix will be controlled

* Corresponding author. Tel.: +33 466 791642; fax: +33 466 797708.
E-mail addresses: jegou@atil.cea.fr, christophe.jegou@cea.fr (C. Jégou).

0022-3115/$ - see front matter © 2005 Elsevier B.V. All rights reserved.
doi:10.1016/j.jnucmat.2005.01.008

by the rate at which uranium is released into the environment. Although uranium is sparingly soluble under reducing conditions similar to those encountered in a repository site, its solubility can increase significantly at the UO_2/water interface because of the α, β, γ irradiation field. Water radiolysis – which produces both oxidizing and reducing species in molecular form (H_2, H_2O_2) or as radicals ($OH^{\bullet}$, e^-_{aq}, $H^{\bullet}$) at concentrations that depend on the nature of the radiation (α or $\beta\gamma$) and on the dose deposited in the water – can lead to the onset of oxidizing conditions at the UO_2/water interface (redox disequilibrium with the environment) and accelerate the dissolution of the spent fuel matrix under disposal conditions [1–3].

The $\beta\gamma$ activity predominates in spent fuel when it is unloaded from the reactor, but diminishes by three orders of magnitude over a millennium and becomes lower than the activity α [1,2]. The latter persists over much longer time periods and must therefore be taken into account over a geological disposal time scale. Spent fuel leaching experiments are not compatible with specific studies of individual radiation sources; an experimental approach is therefore being developed by the CEA to deconvolute these effects. This approach addresses two major issues through:

- leaching experiments on UO_2 fuel pellets doped with alpha-emitters ($^{238/239}Pu$) at various concentrations to reproduce the evolution of the alpha activity in a spent fuel sample with a burnup of 47 GWd t^{-1}_{HM} over 40 000 years [4];
- leaching experiments on UO_2 fuel pellets doped with alpha emitters and on spent fuel irradiated by an external gamma source.

This article presents the main results obtained on the second research topic, although the discussion also draws freely on the previously published results obtained under alpha irradiation alone (first research topic) [4–7].

The objective of these studies is ultimately to quantify the spent fuel UO_2 matrix dissolution rate in order to model its long-term behavior according to the dose rate at the UO_2/water interface and the quantities of oxidizing species generated under irradiation.

2. Experimental

2.1. Materials

Leaching experiments were carried out with two types of materials: UO_2 pellets lightly doped with alpha-emitters, and spent fuel fragments. The objectives were to study the effect of the spent fuel chemistry on UO_2 matrix alteration subjected to gamma irradiation under various conditions, and to obtain data on the combined effect of α, β, γ radiation on oxidizing dissolution of UO_2.

2.1.1. UO_2 pellets doped with alpha-emitters

The leaching experiments under gamma irradiation discussed in this article are part of a broader approach intended to quantify the impact of α, β, γ radiation on oxidizing dissolution of UO_2, and fuel pellets doped with alpha-emitters were used. Pellets were fabricated doped with ^{238}Pu and ^{239}Pu ($0.011\%^{238}Pu + 0.206\%^{239}Pu$ = 0.217 wt% Pu) with an alpha activity of 0.7×10^8 Bq/g_{UO_2} (3.30×10^5 cm^{-2} s^{-1}), equivalent to spent fuel with a burnup of 47 GWd t^{-1}_{HM} 1500 years after disposal [4]. UO_2 powder was impregnated with a nitric acid solution

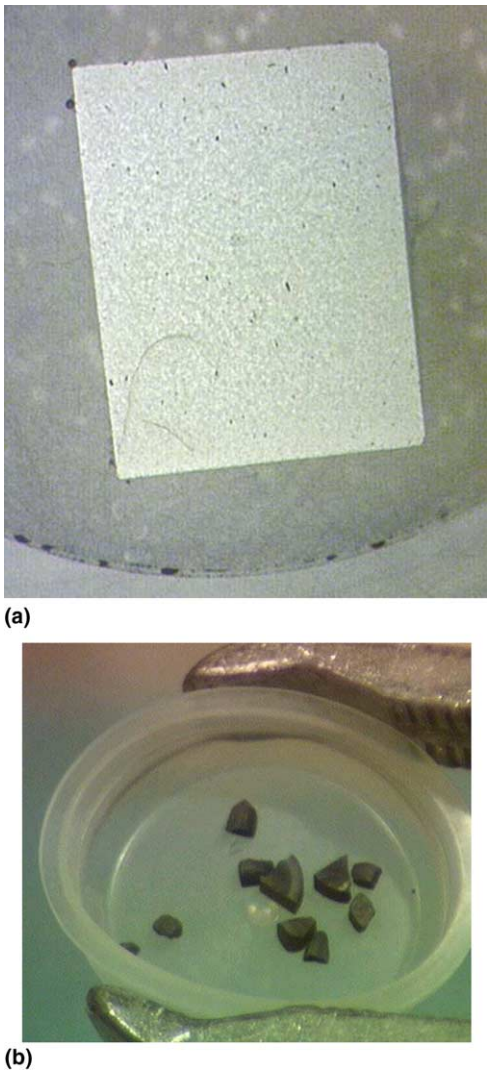

(a)

(b)

Fig. 1. (a) Optical micrograph of UO_2 pellets doped with alpha-emitters (0.7×10^8 Bq/g_{UO2}) (8 mm dia. × 10 mm high). (b) Spent UOX60 fuel fragments (GWd t^{-1}_{HM}).

containing plutonium. After calcining and press compaction, the pellets were sintered for 80 h at 1250 °C under argon atmosphere. Fig. 1(a) shows an optical micrograph of the sintered pellets, 10 mm high and 8 mm in diameter. The measured pellet density (≈97% d_{th}) indicated satisfactory densification. Electron microprobe analysis of the plutonium revealed a uniform plutonium distribution in the UO_2 matrix. For leaching experiments under gamma irradiation, disks 2 mm thick and 8 mm in diameter were cut from the sintered pellets, then polished to a surface roughness of less than one micrometer. The disks were finally annealed for 6 h at 1100 °C in Ar/H_2 to eliminate irradiation damage and guarantee the stoichiometry. The elapsed time between annealing and the gamma irradiation leaching experiments did not exceed a week, and after annealing the pellets were stored under argon atmosphere. The pellets were also preleached before the leaching experiments under gamma irradiation (Section 2.3).

2.1.2. Spent fuel

Leaching experiments were carried out on spent fuel fragments with a burnup of 60 GWd t_{HM}^{-1} (Fig. 1(b)). The fuel (designated UOX60 in the remainder of this article) was initially enriched to 4.5 wt% ^{235}U and irradiated in the French Gravelines 2 reactor for five cycles from November 20, 1983, to May 6, 1989. The fuel radionuclide inventory and thermal power ratings as of the date of the leaching experiments were calculated using the CESAR code [8] (Table 1). The alpha activity of the fragments as of the date of the leaching experiments was 6×10^8 Bq/g_{UO_2}, i.e. 9 times higher than that of the doped UO_2 pellets.

Table 1
Mass fractions of chemical elements and isotopes and thermal power for UOX60 spent fuel, calculated using the CESAR code [8]

Isotope/element	x_i
U	8.15E−01
Pu	1.02E−02
^{236}Pu	7.70E−11
^{237}Pu	6.50E−41
^{238}Pu	3.93E−04
^{239}Pu	5.18E−03
^{240}Pu	2.77E−03
^{241}Pu	8.27E−04
^{242}Pu	1.01E−03
^{243}Pu	8.87E−19
^{244}Pu	1.00E−07
^{241}Am	8.45E−04
^{244}Cm	7.58E−05
Cs	3.52E−03
^{134}Cs	2.05E−06
^{137}Cs	1.32E−03
Eu	1.92E−04
^{154}Eu	1.69E−05
^{155}Eu	2.13E−06
Sr	1.04E−03
^{90}Sr	5.39E−04
^{86}Sr	9.00E−07
^{88}Sr	4.97E−04
^{89}Sr	3.40E−35
Thermal power	W t_{HM}^{-1}
α	6.5E+02
β	7.2E+02
γ	5.5E+02

In this type of fuel with such a high burnup the oxide-cladding gap is fully closed at room temperature [9]: the fuel pellet is 'bonded' to the Zircaloy cladding. For these leaching experiments, fuel fragments were sampled from the middle of a previously leached clad segment (Fig. 1(b)). After sampling, the periphery of the pellet (≈400 μm), i.e. the rim, continued to adhere to the inner face of the cladding. The grain structure of the rim is very different from the structure observed at the pellet core (grain size 1 μm versus 7–10 μm in the core) [10]. This structure is more reactive because of the higher specific surface area (up to 30% porosity); the rim is therefore included in the labile fuel inventory for calculation of the 'labile' source term [3]. The sampling technique and choice of fuel ensure greater control over the fragment surface area accessible to water during leaching, and avoids sampling the rim; this ensures that the study focuses on the actual dissolution of the spent fuel matrix alone.

2.2. Gamma irradiation technique

A 260 Ci ^{60}Co source situated at the center of a cylindrical lead irradiator was used to irradiate a leaching device installed immediately above the source (Fig. 2(a)). Lead shields could be inserted between the bottom of the leaching vessel and the source to modulate the gamma dose rate received by the solution. The gamma dose rates received by the solution as determined by Fricke dosimetry [11] ranged from 650 to 90 Gy h^{-1} depending on the nature and thickness of the shielding (Fig. 2(b)). The leaching device above the source was machined from titanium, and the leaching vessel was fitted with a titanium liner to contain the solution. Both the liner and the titanium sample holder were exposed to a flame to form a passivating TiO_2 film, thus ensuring there would be no interaction between the species generated by water radiolysis and the experimental setup.

2.3. Leaching protocols

2.3.1. Leach tests

For greater clarity, the sample leaching summary is summarized in Fig. 3.

2.3.1.1. Preleaching of spent fuel before gamma irradiation experiment. The clad spent fuel segment from

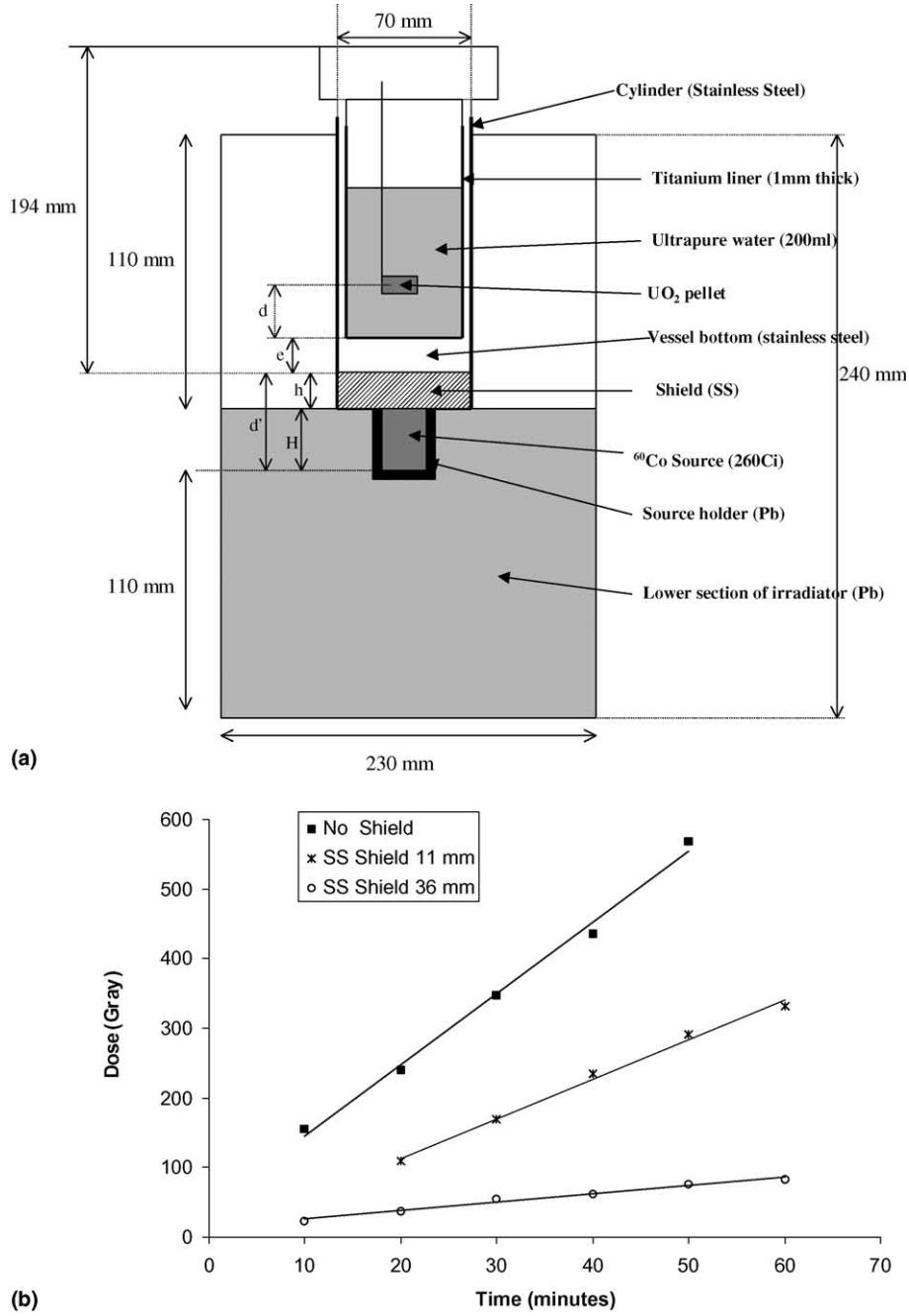

Fig. 2. (a) Overall view of irradiator; (b) dose received by the solution versus time and thickness of stainless steel screens.

which the fragments were sampled was initially leached in pure aerated water for 2 months to eliminate the labile inventory. The sampled fragments were submitted to preleaching cycles before each leaching experiment in a gamma irradiation field. Each 1-hour preleaching cycle was performed in 10 mL of deionized water. The purpose of the preleaching was to avoid a U(VI) release peak due to surface oxidation that could have subsequently masked the radiolysis effects.

2.3.1.2. Preleaching of doped UO_2 before gamma irradiation experiment. Before each gamma irradiation experiment the doped UO_2 was subjected to at least 5 preleaching cycles. Each 1-hour preleaching cycle was

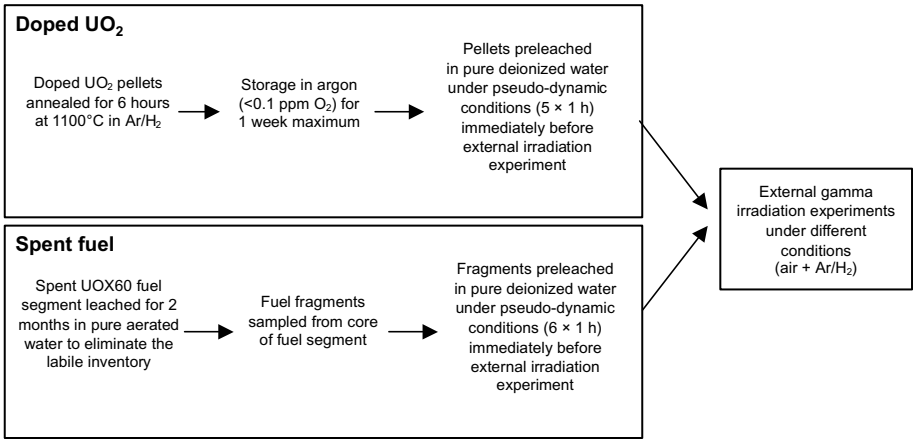

Fig. 3. Specimen leaching history.

performed in 10 mL of deionized water. As for spent fuel the purpose of the preleaching was to avoid a U(VI) release peak due to surface oxidation that could have subsequently masked the radiolysis effects.

2.3.1.3. External gamma irradiation experiments. Four leaching experiments were carried out under external gamma irradiation; the source generated a dose rate of 650 Gy h^{-1} (there was no screen between the source and the leaching vessel).

Table 2 shows the conditions under which the four experiments were carried out. The first two external irradiation experiments were performed on UO_2 pellets doped with alpha-emitters in two types of atmosphere: an aerated medium (a sealed vessel containing water and air) and argon atmosphere (Ar + 4%H_2, <0.1 ppm O_2). The last two experiments were carried out on spent UOX60 fuel fragments under the same two atmospheres as above. Fresh polished and annealed UO_2 pellets were used for experiments 1 and 2; different fuel fragments were used for both experiments 3 and 4.

Leach tests were conducted in a shielded cell at room temperature (25 °C) with deionized water (pH 6.3) in static mode (without solution renewal, $V = 230$ mL). For the experiments under argon atmosphere, the solution was sparged for 6 h before initiating the leaching test. Solution samples were taken over a 16-day period at the following intervals: 1 h, 1, 3, 7, 10 and 14 days). At the end of each experiment the leaching vessel was removed from the irradiator and opened, and the sample was removed from the sample holder. After measuring the leachate pH, 14 N HNO_3 was used to acidify the leachate in the vessel to 0.5 N. The sample holder was also immersed in the acidified solution. After one day of acidification, a sample was taken and the solution was discarded. The vessel was rinsed one last time for 24 h with 230 mL of 0.5 N HNO_3 to solubilize any remaining precipitates or colloids that could have been deposited on the vessel walls or on the sampling rod.

2.3.1.4. Reference experiments. Two reference leaching experiments were carried out on UO_2 disks and on 3 spent UOX60 fuel fragments without external gamma irradiation in aerated media under the same conditions as above. The uranium release was measured after two weeks of leaching.

2.3.2. Solution analysis

Chemical and radiochemical analysis was performed on the liquid test samples to quantify the radionuclide release (U, Pu, Am, Cm, Cs, Sr), and the H_2O_2 analysis generated by radiolysis.

H_2O_2 analysis. Two determination methods were used depending on the H_2O_2 concentrations in the samples.

Table 2
External gamma irradiation experiments (650 Gy h^{-1})

Exp.	Material	Characteristics	Cover gas	Water	S_{geo} (cm^2)	S/V (m^{-1})
1	UO_2 α-doped 0.7×10^8 Bq/g_{UO_2}	2 disks: polished, annealed and preleached	Air	Deionized water	3	1.3
2	UO_2 α-doped 0.7×10^8 Bq/g_{UO_2}	2 disks: polished, annealed and preleached	Ar/H_2 (4%)	Deionized water	3	1.3
3	Spent fuel UOX60	10 preleached fragments	Air	Deionized water	1.5	2 (0.7)
4	Spent fuel UOX60	11 preleached fragments	Ar/H_2 (4%)	Deionized water	1.9	2.4 (0.8)

() without shape factor.

Ghormley's spectrophotometry method [12] was employed for concentrations ranging from 4×10^{-6} to 2×10^{-4} mol L^{-1}; for lower concentrations (1×10^{-9} to 6×10^{-7} mol L^{-1}), chemiluminescence [13] was used in conjunction with a metered additive method [14].

Uranium analysis. Uranium was assayed using a laser-induced kinetic phosphorescence analyzer (KPA). This technique is capable of determining concentrations between 0.5 and 100 μg L^{-1}, i.e. 2.1×10^{-9} to 4.21×10^{-7} mol L^{-1} of uranium.

Strontium analysis. Strontium was analyzed by ICP-AES using a sequential detector. The strontium quantification limit using this technique is 1 μg L^{-1}.

Radiometric analysis. Classical radiometric techniques such as alpha and gamma spectroscopy were used to determine plutonium (^{238}Pu, ^{239}Pu and ^{240}Pu), americium (^{241}Am), curium (^{244}Cm) and cesium (^{134}Cs and ^{137}Cs).

2.4. Solution analysis results

2.4.1. Sample surface area

An important parameter affecting radionuclide release and alteration rate calculations for a solid sample is the surface area, S, in contact with solution [15,16].

In the case of doped UO_2 pellets, the surface area was estimated geometrically from the dimensions of the disks (d = 8 mm and h = 2 mm). Two polished disks (roughness <1 μm) were leached during each gamma irradiation experiment, with a total surface area of S = 3 cm^2. This value represents the reference surface area.

The geometric surface area of the millimeter-size spent fuel fragments was estimated by two methods: one based on photos of each fragment and the other by considering the fragments as spheres; given the mass of each fragment and the fuel density, the surface area was thus easily estimated. For the spent fuel fragments a shape factor of 3 can also be applied to the geometric estimates [15,16]. The shape factor is the main source of uncertainty in calculating the alteration rates and normalized mass losses. The shape factor is not taken into account in the figures and tables indicating the results for the spent fuel, although two rate values (with and without the shape factor) are systematically considered in the discussion.

The S/V ratios were thus comparable for both types of irradiation experiments: 1.3 m^{-1} for doped UO_2 and 2–2.4 m^{-1} (0.7–0.8 m^{-1} without the shape factor) for spent fuel.

2.4.2. Normalized mass losses and alteration rates

The normalized mass loss, $N_L(i)$ (mg m^{-2}) for a chemical element or isotope i is expressed as follows:

$$N_L(i) = \frac{\Delta m_i}{x_i \times S},$$

where Δm_i (mg) is the mass of chemical element or isotope i released into solution as determined by solution analysis, x_i is the mass fraction of element or isotope i in the solid, and S (m^2) is the surface area of the solid.

At sampling interval n, Δm_i (mg) is calculated by summing the quantities sampled up to interval n with the quantity in the leachate at interval n. If C_i is the concentration of a chemical element i in solution, then

$$\Delta m_i = \sum_{j=1}^{n-1} C_i^j V_s^j + C_i^n V_{sol}^n,$$

where j is a sampling interval prior to n, C_i^j is the concentration of element i at interval j, V_s^j is the volume sampled at interval j, C_i^n is the concentration of element i at interval j and V_{sol} is the leachate volume at interval n. It should be noted that the calculated mass loss is thus subject to error in the event of solution evaporation or significant radionuclide sorption. Evaporation was negligible, as the experiments were performed at 25 °C; with regard to sorption, the experimental device components were acid-rinsed at the end of the experiments to correct and interpret the calculated mass losses.

The mass fraction x_i is defined as follows:

$$x_i = \frac{m_i}{m},$$

where m_i is the mass of chemical element or isotope i in the solid with a total mass m. Table 1 indicates the mass fractions of chemical elements and isotopes for the test materials as of the date of the experiments.

The congruence ratio R_{ij} is defined as the ratio of the normalized mass losses for the two species i and j in the solid:

$$R_{ij} = \frac{N_L(i)}{N_L(j)}.$$

The dissolution of radionuclides i and j is termed 'congruent' if R_{ij} = 1 over time.

The dissolution (or leaching) rate normalized for element or isotope i, $R_L(i)$ (mg m^{-2} d^{-1}) is defined as follows if the surface area does not vary over time:

$$R_L(i) = \frac{d}{dt}(N_L(i)) = \frac{1}{x_i \times S} \times \frac{d}{dt}(\Delta m_i).$$

3. Results and discussion

3.1. Gamma irradiation experiments on UO_2 pellets doped with alpha emitters: experiments 1 and 2

3.1.1. Effect of gamma irradiation on UO_2 matrix alteration in aerated media: experiment1

Fig. 4(a) shows the normalized mass loss versus time for the UO_2 pellets. In apparent contradiction with the intermediate sampling results, analysis of the acidified

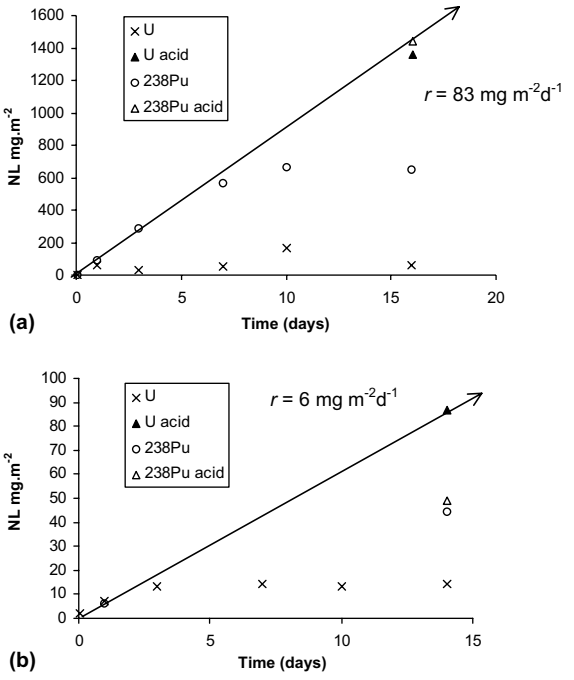

Fig. 4. Normalized mass loss versus time for UO_2 (1500-year batch) subjected to gamma irradiation (650 Gy h^{-1}): (a) in aerated conditions, (b) in Ar + 4%H_2.

leachate (U_{acidif} + $^{238}Pu_{acidif}$) showed that pellet dissolution was linear over time under these alteration conditions. The alteration rate ($R_L(U)$ = 83 mg m^{-2} d^{-1}) was much higher than under similar alteration conditions without irradiation (UO_2 reference experiment). The uranium concentration in the acidified leachate without gamma irradiation was 8.7 μg L^{-1} (Table 3) compared with 1777 μg L^{-1} under irradiation (Table 4). The average rate determined without irradiation was about $R_L(U)$ = 0.5 mg m^{-2} d^{-1}, i.e. lower by a factor of 170. The rate determined experimentally under gamma irradiation was of the same order of magnitude as the value proposed by Sunder ($R_L(U)$ = 30 mg m^{-2} d^{-1}) [17] for UO_2 with a gamma dose rate of 600 Gy h^{-1} and without alpha irradiation.

^{238}Pu exhibited leaching behavior congruent with uranium as determined from the data obtained after acidification of the leachate (Table 5). This congruence confirms that Pu was homogeneously distributed in the UO_2 pellets and suggests that Pu release is indeed controlled by alteration of the UO_2 matrix.

3.1.2. Effect of the cover gas (air or Ar + H_2) on UO_2 matrix alteration: experiment 2

Fig. 4(b) shows the evolution of the normalized uranium mass loss over time. As for experiment 1, and in apparent contradiction with the intermediate samples, analysis of the acidified leachate at the end of the experiment showed that the pellet alteration kinetics were linear over time. The alteration rate determined by linear regression of the normalized mass losses was 6 mg m^{-2} d^{-1} under the conditions of experiment 2. Comparing experiments 1 and 2 shows that under external gamma irradiation (650 Gy h^{-1}), the atmosphere and the dissolved oxygen concentration in solution have an influence on alteration: the uranium dissolution rate under deaerated conditions ($R_L(U)$ = 6 mg m^{-2} d^{-1}, $[O_2] = 1.2 \times 10^{-10}$ mol L^{-1}) was 15 times lower than in air ($R_L(U)$ = 83 mg m^{-2} d^{-1}, $[O_2] = 2.5 \times 10^{-4}$ mol L^{-1}). The uranium dissolution rate in deaerated media under gamma irradiation was still substantially higher (by a factor of 12) than the rate without irradiation in aerated media (reference experiment) (Table 3).

3.1.3. H_2O_2 production under gamma irradiation: experiments 1 and 2

Experimental data. In order to account for the differences in the alteration kinetics with the experimental conditions, the quantities of oxidizing species – especially hydrogen peroxide generated by gamma radiolysis of water – were determined experimentally. Radiologically induced oxidizing species ($O_2^{\bullet-}$, $OH^{\bullet}$, H_2O_2, O_2, etc.) attack and dissolve the UO_2 matrix according to the mechanism of oxidizing dissolution [2,17]. Fig. 5 shows that significant differences were observed: the steady-state H_2O_2 concentration was 1.2×10^{-4} mol L^{-1} in the aerated medium versus 3.2×10^{-8} mol L^{-1} in Ar + 4%H_2. Although radiation with low linear energy transfer (LET), such as gamma radiation, produces a large number of primary radicals and a small number of primary molecular products such as H_2O_2 [17], the

Table 3
Reference experiments on UO_2 (2 polished disks) and UOX60 (3 fragments) in pure water and in aerated medium

Time	UO_2 S/V = 1.3 m^{-1}			UOX 60 S/V = 0.9 m^{-1}		
	[U] (μg/L)	[U] (mol/L)	NL(U) (mg/m^2)	[U] (μg/L)	[U] (mol/L)	NL(U) (mg/m^2)
1 h				0.9	3.8E−9	0.96
1 day				2.9	1.2E−8	3.10
5 days	1.43	6.03E−9	1.25	9	3.8E−8	9.64
14 days	2.05	9.86E−9	2.05			
14 days (acidification)	8.74	3.67E−8	7.62	16	6.7E−8	17.14

Table 4
Results of leaching experiments 1 and 2

	[U] (μg/L)	[U] (mol/L)	NL(U) (mg/m^2)	[^{238}Pu] (Bq/m L)	[^{238}Pu] (mol/L)	NL(^{238}Pu) (mg/m^2)	R(^{238}Pu/U)	[^{239}Pu] (Bq/m L)	[^{239}Pu] (mol/L)	NL(^{239}Pu) (mg/m^2)	R(^{239}Pu/U)
Air											
0	0.01			0.1				0.20			
1 h	3.7	1.55E−08	2.84	0.2	1.33E−12	2.42	0.85	<QL	nd	nd	nd
1 day	67	2.82E−07	63	7.7	5.10E−11	90	1.44	<QL	nd	nd	nd
3 days	31	1.30E−07	30	25	1.66E−10	284	9.48	<QL	nd	nd	nd
7 days	57	2.39E−07	56	52	3.45E−10	564	10.08	0.9	1.64E−09	145	2.59
10 days	199	8.36E−07	164	63	4.17E−10	665	4.05	0.6	1.09E−09	97	0.59
16 days	69	2.90E−07	61	64	4.24E−10	648	10.67	5.5	1.00E−08	772	12.71
16 days (acidification)	1777	7.47E−06	1294	153	1.01E−09	1389	1.07	5.8	1.06E−08	858	0.66
16 days (rinse)	44	1.85E−07	1335	4.4	2.92E−11	1441	1.08	0.4	7.28E−10	929	0.70
Ar/H_2 (4%)											
0	0.09			0.04				0.09			
1 h	2.44	1.03E−08	2	0.57	3.78E−12	6	2.94	1.80	3.28E−09	280	137
1 day	8.75	3.68E−08	7	<QL	nd	nd	nd	<QL	nd	nd	nd
3 days	16.75	7.04E−08	13	0.11	7.29E−13	1	0.10	0.26	4.73E−10	48	3.62
7 days	18.18	7.64E−08	14	<QL	nd	nd	nd	<QL	nd	nd	nd
10 days	16.90	7.10E−08	13	<QL	nd	nd	nd	<QL	nd	nd	nd
14 days	18.88	7.93E−08	15	<QL	nd	nd	nd	<QL	nd	nd	nd
14 days (acidification)	92.62	3.89E−07	85	3.94	2.61E−11	44	0.52	1.34	2.43E−09	234	2.74
14 days (rinse)	1.52	6.39E−09	87	0.40	2.62E−12	49	0.56	0.17	3.10E−10	262	3.02

Table 5
Primary radiolytic yields and kinetic diagram for water radiolysis (without uranium)

Reaction	Rate constant ($d\ m^3\ mol^{-1}\ s^{-1}$)
RE1: OH + H_2 = H_2O + H	k = 3.4E7
RE2: OH + H_2O_2 = H_2O + HO_2	k = 2.7E7
RE3: OH + O_2[−] = OH[−] + O_2	k = 1.0E10
RE4: OH + HO_2 = H_2O + O_2	k = 7.1E9
RE5: OH + OH = H_2O_2	k = 5.5E9
RE6: OH + OH[−] = H_2O + O[−]	k = 1.2E10
RE7: OH + HO_2[−] = HO_2 + OH[−]	k = 7.5E9
RE8: OH + H = H_2O	k = 7.0E9
RE9: OH + E[−] = OH[−] + H_2O	k = 3.1E10
RE10: OH + O[−] = HO_2[−]	k = 1.8E10
RE11: O[−] + H_2O = OH + OH[−]	k = 1.7E6
RE12: E[−] + O_2 = O_2[−] + H_2O	k = 1.9E10
RE13: E[−] + H_2O_2 = OH[−] + OH + H_2O	k = 1.1E10
RE14: E[−] + O_2[−] = HO_2[−] + OH[−]	k = 1.3E10
RE15: E[−] + H[+] = H + H_2O	k = 2.3E10
RE16: E[−] + H_2O = H + OH[−] + H_2O	k = 1.9E1
RE17: E[−] + HO_2[−] = O[−] + OH[−] + H_2O	k = 3.5E9
RE18: E[−] + E[−] = H_2 + 2 * OH[−]	k = 5.5E9
RE19: E[−] + HO_2 = HO_2[−] + H_2O	k = 2.0E10
RE20: E[−] + H = H_2 + OH[−]	k = 2.5E10
RE21: H + HO_2 = H_2O_2	k = 2.0E10
RE22: H + H_2O_2 = H_2O + OH	k = 9.0E7
RE23: H + OH[−] = E[−]	k = 2.2E7
RE24: H + O_2 = HO_2	k = 2.1E10
RE25: H + O_2[−] = HO_2[−]	k = 2.0E10
RE26: H + H = H_2	k = 7.8E9
RE27: HO_2 + O_2[−] = O_2 + HO_2[−]	k = 9.6E7
RE28: HO_2 + HO_2 = H_2O_2 + O_2	k = 8.4E5
RE29: HO_2 = H[+] + O_2[−]	k = 8.0E5
RE30: H[+] + O_2[−] = HO_2	k = 5.0E10
RE31: H[+] + HO_2[−] = H_2O_2	k = 2.0E10
RE32: H_2O_2 = H[+] + HO_2[−]	k = 3.56E−2
RE33: H[+] + OH[−] = H_2O	k = 1.43E11
RE34: H_2O = H[+] + OH[−]	k = 2.6E−5
RE35: O_2[−] + O_2[−] = HO_2[−] + O_2–H[+]	k = 1.8E9

Species	Gamma (G value molecules/100 eV)
$OH^{\bullet}$	2.67
e^-_{aq}	2.66
$H^{\bullet}$	0.55
H_2	0.45
H_2O_2	0.72
H^+	2.76
OH^-	0.1
$HO_2^{\bullet}$	0
$-H_2O$	6.87

The kinetic constants are defined at 25 °C [16].

nature of the cover gas can considerably modify the steady-state concentrations of the molecular species in the homogeneous solution [18]. The presence of oxygen accelerates the decomposition of water into molecular products in particular [18] since it very effectively captures e^-_{aq} electrons and H atoms according to the following mechanism:

$$e^-_{aq} + O_2 \rightarrow O_2^{\bullet -}$$

$$H^{\bullet} + O_2 \rightarrow HO_2^{\bullet}$$

The superoxide ion $O_2^{\bullet -}$, its protonated form, and the hydroperoxyl radical react together to form hydrogen peroxide and oxygen, or with $OH^{\bullet}$ to form only oxygen.

$$O_2^{\bullet -} + HO_2^{\bullet}(+H_2O) \rightarrow \mathbf{H_2O_2} + \mathbf{O_2} + OH^-$$

$$2HO_2^{\bullet} \rightarrow H_2O_2 + O_2$$

$$O_2^{\bullet -} + OH^{\bullet} \rightarrow O_2 + OH^-$$

$$HO_2^{\bullet} + OH^{\bullet} \rightarrow \mathbf{O_2} + H_2O$$

The significant H_2O_2 production measured in the aerated media experiments partially accounts for the uranium release observed in experiment 1 compared with experiment 2. The oxidizing species produced by irradiation nevertheless also had a role in experiment 2 since the alteration rate determined in this case was higher than without gamma irradiation in aerated media (reference experiment). Moreover, the radicals played a major role compared with H_2O_2 in experiment 2 since the uranium dissolution rate under gamma irradiation was several orders of magnitude higher than measured during an experiment in which hydrogen peroxide was added to a solution that was not exposed to any radiation field [17].

Radiolysis calculations in pure water and under gamma radiation. The Chemsimul kinetic code [19] was used to calculate the evolution of the H_2O_2 concentrations in the homogeneous solution and the steady-state concentration. The chemical reactions and kinetic constants are indicated in Table 5 together with the primary radiolytic yields used under gamma irradiation. Fig. 5 shows very close agreement between the calculated and experimentally measured steady-state concentrations. A simple calculation of the H_2O_2 concentration obtained in the homogeneous solution under γ irradiation without allowing for interaction with the UO_2 pellet surface was able to reproduce the experimental results. Even if hydrogen peroxide is consumed at the UO_2/water interface, steady-state conditions in the homogeneous solution are not modified by the presence of UO_2 pellets. This result is not surprising in the light of calculations by Christensen [19–22] and Jégou [4], if it is assumed that only molecular species within 100 μm of the UO_2/water interface can take part in oxidizing dissolution

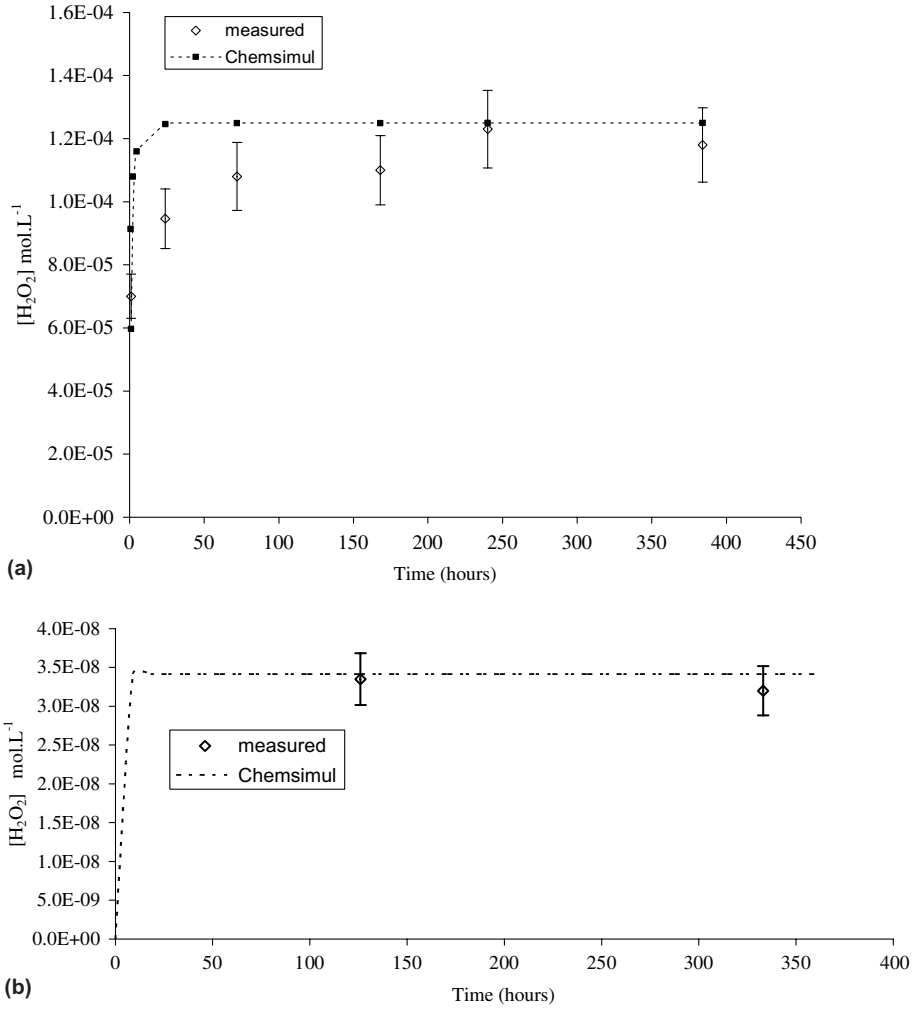

Fig. 5. Hydrogen peroxide concentration in the homogeneous solution versus time in air and in Ar + 4%H_2 (experiments 1 and 2).

of the UO_2 matrix. Water radiolysis calculations in the homogeneous phase also show (Table 6) significant differences in the concentrations of oxidizing radicals depending on the nature of the cover gas: the $O_2^{\bullet -}$ and $HO_2^{\bullet}$ concentrations drop by several orders of magnitude in the presence of Ar + 4%H_2. The mean free path of these species is short (about 13 μm at 650 Gy h^{-1} [20]), and only those situated extremely close to the surface are likely to oxidize UO_2.

3.1.4. Combined effects of α and γ irradiation on UO_2 matrix alteration

Regardless of the cover gas (air or Ar + 4%H_2) the alteration rates measured in a mixed alpha and gamma irradiation field ($\dot{D}\gamma = 650$ Gy h^{-1}) remain higher than under the effect of the alpha irradiation field alone for the UO_2 sample ($\dot{D}\alpha = 110$ Gy h^{-1}; flux = 3.30×10^5 α cm^{-2} s^{-1}). Leaching experiments on doped UO_2 pellets from a single batch, in pure water ($S/V = 3$ m^{-1}) for one month in a deaerated medium (Ar with <0.1 ppm O_2) resulted in low uranium concentrations (10 μg L^{-1}) on completion of the test, corresponding to a mean alteration rate of 0.2 mg m^{-2} d^{-1} [4] under alpha radiolysis alone. This rate is 415 to 30 times lower than obtained under gamma irradiation in air and in Ar + 4%H_2. Moreover, no traces of H_2O_2 were detected in these experiments [4] investigating alpha irradiation, unlike the gamma irradiation experiments described in this article.

Sattonnay [23] obtained results for uranium release from the UO_2/water interface under intense external alpha irradiation (3.30×10^{10} α cm^{-2} s^1) that generated 4.8×10^{-4} mol L^{-1} H_2O_2 in the homogeneous solution ($S/V = 2.8$ m^{-1}), compared with the results of experiment1, which generated 1.2×10^{-4} mol L^{-1} H_2O_2 in the homogeneous solution ($S/V = 1.3$ m^{-1}); the 1-hour

Table 6
Concentrations of radicals and molecular species calculated using the Chemsimul code [19] after 14 days of gamma irradiation (650 Gy h^{-1}) in the homogeneous solution in air and in Ar + 4%H_2

Medium	Concentrations of species (mol L^{-1})								
	OH·	H_2	H·	H_2O_2	$HO_2^{\cdot}$	$O_2^{-\cdot}$	O_2	O^-	HO_2^-	e^-
Aerated										
Water radiolysis (γ = 650 Gy h^{-1})	1.6×10^{-11}	1.55×10^{-5}	4.56×10^{-15}	1.25×10^{-4}	3.58×10^{-11}	5.48×10^{-9}	1.95×10^{-4}	3.56×10^{-18}	2.16×10^{-9}	9.78×10^{-15}
Ar + 4%H_2										
Water radiolysis (γ = 650 Gy h^{-1})	5.9×10^{-11}	$3.12\ 10^{-5}$	2.6×10^{-9}	3.4×10^{-8}	6.55×10^{-15}	1.03×10^{-12}	1.1×10^{-14}	1.36×10^{-17}	6.33×10^{-13}	1.46×10^{-11}

release was much greater under external alpha irradiation. The uranium concentration obtained by Sattonnay [23] was 210 μg L^{-1} versus 3.7 μg L^{-1} for experiment 1. Even though the H_2O_2 concentrations in the homogeneous solution were comparable both types of experiments under irradiation, the alpha irradiation localized in the 35–40 μm of water at the surface of the pellet and the existence of strong H_2O_2 concentration gradients between the homogeneous solution and the interface under high alpha flux could account for the observed differences in behavior.

3.1.5. pH variation under irradiation and actinide behavior

3.1.5.1. pH variation. No variation in the pH was observed for experiments in Ar + 4%H_2 (experiment 2) whereas the pH diminished slightly from 6.3 (±0.2) to 5.8 (±0.2) in air (experiment 1). Several mechanisms, including the formation of nitric acid under gamma irradiation [24,25], precipitation of a secondary phase [23], a return to equilibrium with the CO_2 partial pressure of the air (pH_{eq} = 5.4 if $P_{CO_2} = 10^{-3.5}$ atm), could account for the acidification of the leachate and warrant further discussion.

Concerning the formation of nitric acid, and Gray and McVay [24] observed the formation of HNO_3 in an air/water system under gamma radiation only when a gaseous phase was present, demonstrating that the reaction must also be initiated in the gaseous phase. Reactions between water radiolysis products and dissolved nitrogen in solution apparently do not generate nitrogen compounds because of their slow kinetics [24,25]. We verified this assumption by three gamma irradiation experiments in our experimental setup without leachable material over a 2-week period at various solution volume to gas volume ratios. The pH measured at the end of the tests (Table 7 and Fig. 6) shows distinct solution acidification when $V_{gas}/V_{liq} = 10$ (pH = 4.1), whereas it was less significant when $V_{gas}/V_{liq} = 1$ (pH = 5.2). Conversely, no acidification arising from the formation of nitric acid was obtained under our experimental conditions: pH = 6.3 and $V_{gas}/V_{liq} = 0.1$. We therefore reduced the gas volume relative to the solution volume in our gamma irradiation experiments to avoid the effects due to nitrogen in the air.

With regard to secondary phase precipitation, the optical micrograph (Fig. 7) of the doped UO_2 pellets

Table 7
pH of the homogeneous solution subjected to gamma irradiation ($\dot{D}\gamma = 650$ Gy h^{-1}) versus gas phase volume to water volume ratio

V_{gas}/V_{liq}	pH	$[H_2O_2]$ (mol L^{-1})
0.1	6.3	1.2×10^{-4}
1	5.2	nd
10	4.1	nd

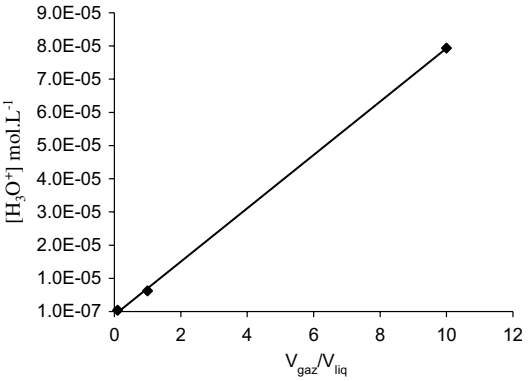

Fig. 6. Hydronium ion concentration in the homogeneous solution under gamma irradiation (650 Gy h^{-1}) versus gas volume to solution volume ratio.

after experiment 1 reveals the presence of phases distributed nonuniformly over the surface that could not be identified by X-ray diffraction. An additional experiment was carried out to identify and enhance the formation of this phase by extended leaching under gamma irradiation in aerated media. X-ray diffraction analysis this time revealed the presence of uranium peroxide (studtite) on the pellet surface (Fig. 7).

Thermodynamic calculations were also performed to provide a few indications of their nature, in view of the experimental U and H_2O_2 concentration data and the pH values for experiments 1 and 2. These calculations were obviously of limited scope and the results are purely indicative given that they assume thermodynamic equilibrium and disregard the irradiation and the redox disequilibrium that could generate metastable species.

The H_2O_2 concentrations (1.2×10^{-4} mol L^{-1}) in the homogeneous solution under gamma irradiation in an aerated medium (experiment 1) appear compatible with the precipitation of uranium peroxide as reported in several studies [23,26] with UO_2. The precipitation reaction is generally defined thus

$$UO_2^{2+} + H_2O_2 \rightarrow UO_4 + 2H^+$$

and the solubility product corresponding to this reaction at room temperature is $K_s = 1.5 \times 10^{-3}$ [23,26]. This reaction releases protons and could thus lead to acidification of the leachate as described by Sattonnay [23], who observed a pH drop under alpha irradiation with an H_2O_2 concentration of 4.8×10^{-4} mol L^{-1}. For

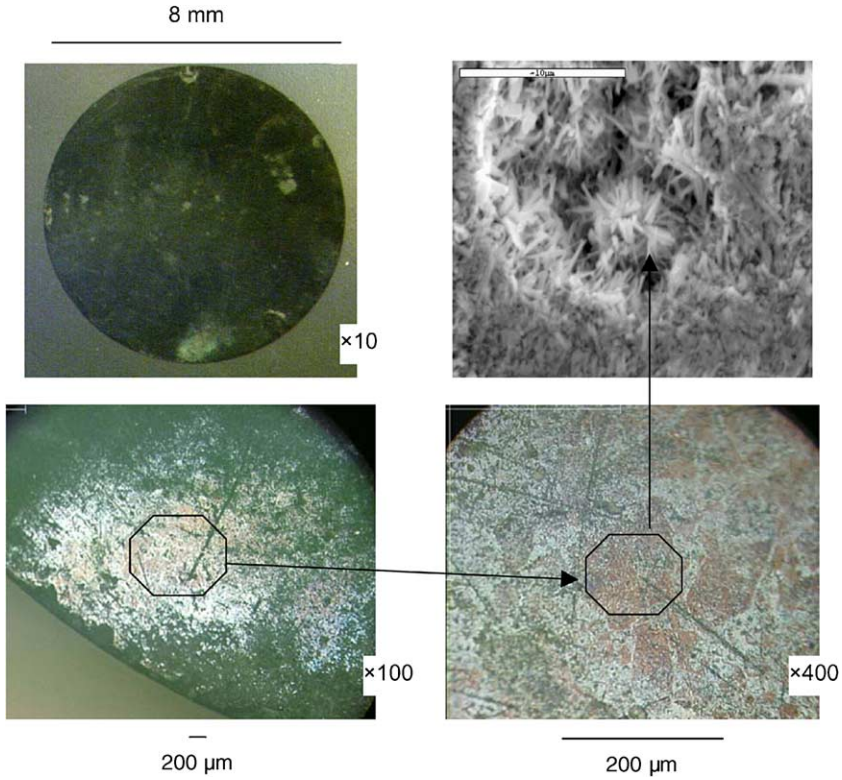

Fig. 7. Studtite deposited on Pu-doped UO_2 pellets after leaching under gamma irradiation (650 Gy h^{-1}) in air (experiment 1).

experiment 1 it is easily verified that the activity product $Q \gg K_s$:

$$\log \frac{\left[UO_2^{2+}\right][H_2O_2]}{[H^+]^2} = 2.7,$$

$$\overline{K_s}$$

where $[UO_2^{2+}] = 1.4 \times 10^{-8}$ mol L^{-1}, $[H_2O_2] = 1.2 \times 10^{-4}$ mol L^{-1} and $[H^+] = 1.6 \times 10^{-6}$ mol L^{-1}.

The UO_2^{2+} ion concentration was estimated from the total uranium concentration in the leachate, i.e. 3.5×10^{-7} mol L^{-1} on average prior to acidification, by speciation computations using the JCHESS calculation code [27] and the thermodynamic database of the EQ3/6 code [28]. The majority aqueous species in pure water (no complexant additive), in oxidizing media at pH = 5.8 is clearly $UO_2(OH)_2$(aq) (Fig. 8) [29]. UO_2CO_3(aq) was a very minor species: assuming a CO_2(g) partial pressure of $10^{-3.5}$ atm in the calculation yielded a UO_2CO_3(aq) concentration of 1.8×10^{-8} mol L^{-1}.

Precipitation could thus have contributed to the slight acidification observed in experiment 1. Note that the low H_2O_2 and uranium concentrations of experiment 2 preclude any precipitation of uranium peroxide [26].

Finally, the precipitation observed during experiment 1 implies that the uranium dissolution rate determined from the solution chemistry underestimates the matrix alteration rate despite the observed linear release conditions, which probably reflect steady-state conditions between the matrix alteration rate and the studtite precipitation rate.

3.1.5.2. Uranium concentrations. The uranium concentrations stabilized at about 3.5×10^{-7} mol L^{-1} for experiment 1 under gamma irradiation in air, and 7×10^{-8} mol L^{-1} for experiment 2 in Ar + 4%H_2. These concentrations were below the solubility of schoepite $UO_2(OH)_2 \cdot H_2O$(s), which in aerated media is about 5×10^{-6} mol L^{-1} [30]. Concerning the possibility that the uranium concentration is controlled by phases such as U_3O_8, U_3O_7, or U_4O_9, for which the solubility diminishes with the redox potential [29,30], the lack of experimental redox data makes such an equilibrium difficult to establish. Satisfactory congruence was observed between plutonium and uranium after acidification leachate, suggesting the presence of actinide coprecipitates likely to have a significant effect on the solubility values.

3.2. Gamma irradiation experiments on spent fuel: experiments 3 and 4

3.2.1. Effect of gamma irradiation on spent fuel matrix alteration in aerated media: experiment 3

3.2.1.1. Actinide behavior. Fig. 9 shows the normalized uranium and plutonium (^{238}Pu) mass losses over time for spent fuel subjected to an external gamma irradiation field ($\dot{D}\gamma(^{60}\text{Co}) = 650$ Gy h^{-1}) in aerated water. As for the UO_2 pellets, leachate acidification on completion of

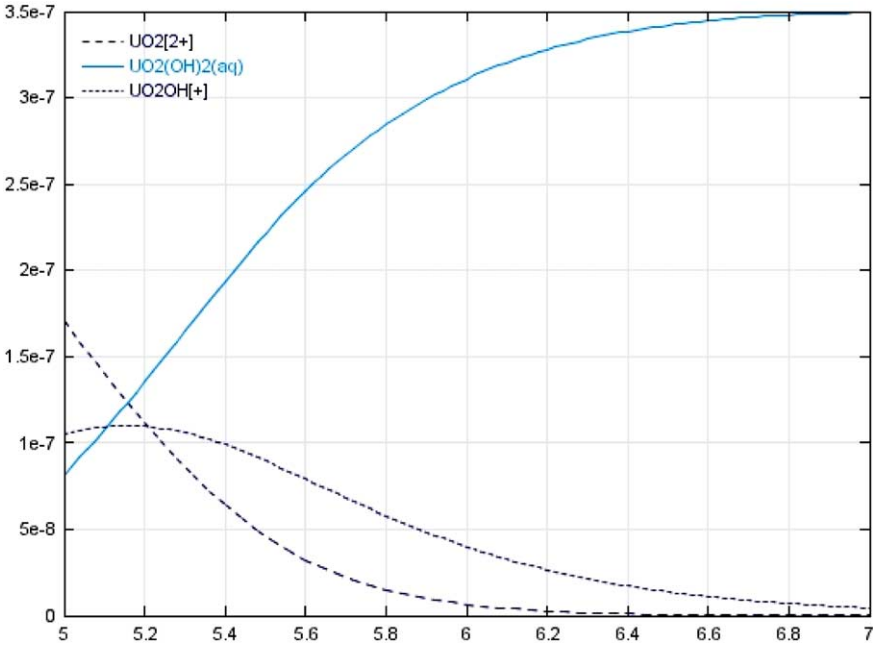

Fig. 8. Uranium speciation ($[U_{tot}] = 3.5 \times 10^{-7}$ mol L^{-1}) in deionized water and in aerated medium versus pH calculated using the JCHESS calculation code [27].

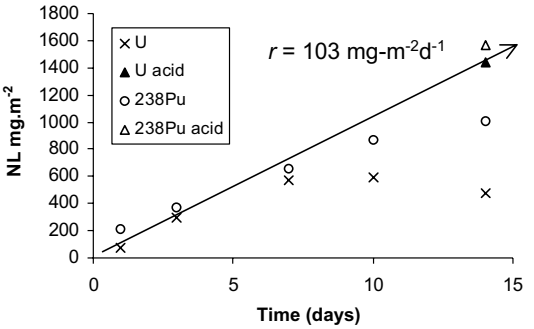

Fig. 9. Normalized mass lossfor U and ^{238}Pu (without allowance for the shape factor of 3) versus time for UOX60 fuel subjected to external gamma irradiation (650 Gy h^{-1}) in aerated medium.

the test resulted in higher normalized mass losses and is indicative of linear alteration of the fragments over time. Good congruence was noted between uranium and the other actinides (^{238}Pu, ^{239}Pu, ^{241}Am, ^{244}Cm) after acidification (Table 8), indicating that their release into solution is indeed controlled by dissolution of the UO_2 fuel matrix. The uranium dissolution rate R_L(U) of the fragments obtained by linear regression of the normalized uranium mass losses was 34 mg m^{-2} d^{-1} (103 mg m^{-2} d^{-1} if the shape factor is disregarded). This rate is fully comparable to the value obtained for doped UO_2 pellets (experiment 1) under the same alteration conditions (aerated medium and $\dot{D}\gamma(^{60}\mathrm{Co}) = 650$ Gy h^{-1}). The uranium dissolution rate determined under the conditions of experiment 1 was 83 mg m^{-2} d^{-1}.

Concerning the mass balance, a comparison between the mass loss values determined by weighing (before and after leaching) and by solution analysis – notably the actinide concentrations after acid rinsing – indicated an 85% recovery factor.[1] The acid rinsing procedure following the experiments thus provides satisfactory mass balances that can be used to determine the mean release rates over the irradiation period.

3.2.1.2. Fission product behavior. For the fission products (Sr, ^{134}Cs and ^{137}Cs) the congruence ratios N_L(Sr)/N_L(U) and $N_L(^{134/137}\mathrm{Cs})/N_L$(U) remained above 10 throughout the irradiation experiment (Table 9). The $N_L(^{134/137}\mathrm{Cs})/N_L$(Sr) ratio was near 1 over the duration of experiment 3. This result indicates that cesium and strontium are satisfactory spent fuel matrix alteration tracers considering the fragment preleaching history. Fig. 10 shows the Cs and Sr releases during the rinsing cycles for spent fuel fragments from two different clad segments: one previously leached for two months (as in the case of the fragments used for this study) and the other without prior leaching. The Cs/U and Sr/U congruence ratios clearly differ by more than an order of magnitude in the fragments taken from a previously unleached segment, highlighting the major contribution of labile inventories in the different source terms and fission product releases. It is therefore unlikely that a major contribution by the labile inventories would have resulted in a $N_L(^{134/137}\mathrm{Cs})/N_L$(Sr) ratio near 1 in the case of experiment 3, performed under gamma irradiation in aerated conditions. The release rates obtained by linear regression of the normalized mass losses (Fig. 11) were 295 and 312 mg m^{-2} d^{-1} for strontium and cesium, respectively (885 and 935 mg m^{-2} d^{-1} if the shape factor is disregarded). These rates are an order of magnitude higher than the actinide release rates, implying that 90% of the actinides precipitated on the surface of the fragments during the leach test. The alteration rates obtained with doped UO_2 pellets in experiment1 were thus significantly underestimated, as suggested by the uranium peroxide precipitates observed on the pellet surface.

3.2.2. Effect of the cover gas (air or Ar + H_2) on spent fuel matrix alteration: experiment 4

3.2.2.1. Actinide behavior. As in experiment 3, satisfactory congruence was observed for all the actinides (Table 10). The mass losses obtained after acid rinsing ranged from 260 to 290 mg m^{-2} for uranium and for the different plutonium isotopes. The mean release rates obtained after 14 days of gamma irradiation were 6.5 mg m^{-2} d^{-1} (20 mg m^{-2} d^{-1} if the shape factor is disregarded). They were slightly higher than the values obtained for doped UO_2 pellets leached under the same experimental conditions (experiment 2) and lower in Ar + 4%H_2 than in air.

3.2.2.2. Fission product behavior. The mass losses for ^{137}Cs and ^{134}Cs after 14 days of leaching were 1380 and 1100 mg m^{-2}, respectively, corresponding to release rates of 33 and 27 mg m^{-2} d^{-1} (100 and 80 mg m^{-2} d^{-1} if the shape factor is disregarded). As in experiment 3, they were significantly higher (by a factor of 5) than the actinide release rates. Since the fragments used for this experiment had been previously leached in the same way as those of experiment 3, it is reasonable to consider cesium as a satisfactory matrix alteration tracer; this suggests that 80% of the actinides reprecipitated on the surface of fragments under these experimental conditions. ICP-AES analysis of strontium revealed concentrations within the determination limits of the analysis method (1 μg L^{-1}) but the estimated mass losses were also compatible and congruent with those observed for cesium (Table 11).

The effect of the cover gas was revealed by a drop in the cesium release rate (by a factor of 10) in the presence

[1] Δm (solution analysis after acid rinsing)/Δm (fragments weighed before and after leaching) × 100.

Table 8
Results of leaching experiment 3: actinide release

Air	[U] (μg/L)	[U] (mol/L)	NL(U) (mg/m^2)	[^{238}Pu] (Bq/mL)	[^{238}Pu] (mol/L)	NL(^{238}Pu) (mg/m^2)	R(^{238} Pu/U)	[^{239}Pu] (Bq/mL)	[^{239}Pu] (mol/L)	NL(^{239}Pu) (mg/m^2)	R(^{239}Pu/U)
0	0			2				0			
1 h	0.25	1.05E−09	0.5	<QL	nd	nd	nd	0.34	6.15E−10	42	
1 day	43	1.82E−07	76	37	2.45E−10	213	2.79	4.39	7.99E−09	531	6.96
3 days	175	7.36E−07	301	66	4.37E−10	373	1.24	2.03	3.69E−09	253	0.84
7 days	342	1.44E−06	572	120	7.95E−10	657	1.15	6.41	1.17E−08	743	1.30
10 days	358	1.50E−06	592	162	1.07E−09	868	1.47	8.44	1.54E−08	957	1.62
14 days	287	1.20E−06	476	192	1.27E−09	1008	2.12	9.12	1.66E−08	1017	2.13
14 days (acidification)	708	2.97E−06	1441	231	1.53E−09	1572	1.09	11.48	2.09E−08	1649	1.14
14 days (rinse)											

Air	[^{240}Pu] (Bq/mL)	[^{240}Pu] (mol/L)	NL(^{240}Pu) (mg/m^2)	R(^{240}Pu/U)	[^{241}Am] (Bq/mL)	[^{241}Am] (mol/L)	NL(^{241}Am) (mg/m^2)	R(^{241}Am/U)	[^{244}Cm] (Bq/mL)	[^{244}Cm] (mol/L)	NL(^{244}Cm) (mg/m^2)	R(^{244} Cm/U)
0	0								2			
1 h	0.66	3.28E−10	42	nd					<QL	nd	nd	nd
1 day	8.61	4.27E−09	533	6.98					9	1.23E−11	57	0.74
3 days	3.98	1.97E−09	253	0.84					<QL	nd	nd	nd
7 days	12.59	6.24E−09	746	1.30					<QL	nd	nd	nd
10 days	16.56	8.21E−09	960	1.62					5	6.84E−12	31	0.05
14 days	17.89	8.87E−09	1021	2.14					<QL	nd	nd	nd
14 days (acidification)	22.53	1.12E−08	1656	1.15	84.20	2.75E−09	1274	0.88	311	1.37E−12	2134	1.48
14 days (rinse)												

Table 9
Results of leaching experiment 3: Fission product release

Air	[^{137}Cs] (Bq/mL)	[^{137}Cs] (mol/L)	NL(^{137}Cs) (mg/m^2)	R (^{137}Cs/U)	[^{134}Cs] (Bq/mL)	[^{134}Cs] (mol/L)	NL(^{134}Cs) (mg/m^2)	R (^{134}Cs/U)	[Sr] (μg/L)	[Sr] (mol/L)	NL(Sr) (mg/m^2)	R (Sr/U)
0												
1 h	194	4.42E−10	68	148.5					2.6	2.89E−08	3692	
1 day	7040	1.60E−08	2378	31.13	198	3.09E−11	2461	32.21	4.1	4.56E−08	5748	75.25
3 days	16920	3.86E−08	5589	18.58	408	6.37E−11	4971	16.52	4.8	5.33E−08	6650	22.10
7 days	32200	7.34E−08	10326	18.06	762	1.19E−10	9009	15.76	8.3	9.22E−08	11062	19.35
10 days	42400	9.66E−08	13334	22.53	1020	1.59E−10	11816	19.97	9.9	1.10E−07	12952	21.89
14 days	53400	1.22E−07	16401	34.43	1174	1.83E−10	13341	28.01	9.6	1.07E−07	12451	26.14
14 days (acidification)	44400	1.01E−07	18254	12.66	956	1.49E−10	14565	10.10	8.3	9.22E−08	14292	9.91
14 days (rinse)									1.9	2.11E−08	17064	11.84

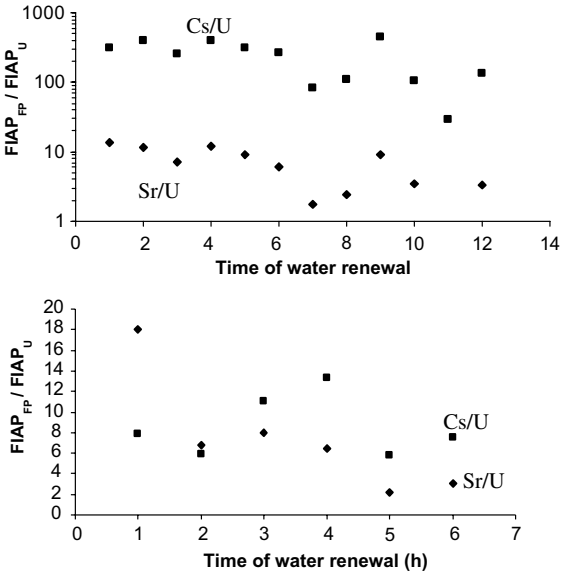

Fig. 10. Cs/U and Sr/U congruence ratios during rinsing cycles on spent UOX60 fuel fragments sampled from a segment from which the labile inventory had not been washed (top) and from a segment previously leached for two months in pure aerated water before sampling the fragments (bottom).

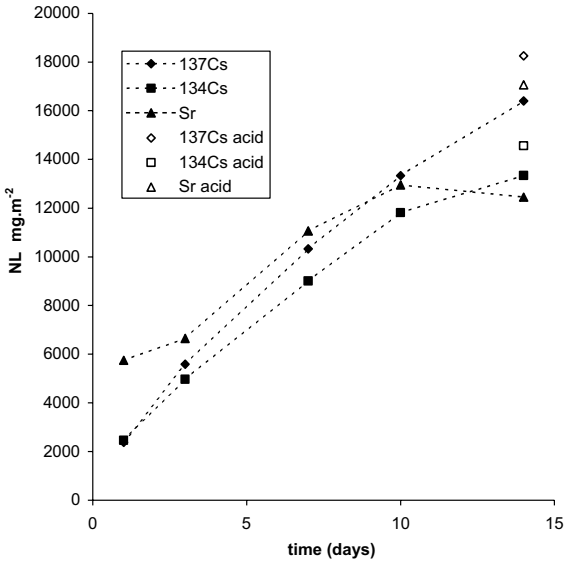

Fig. 11. Normalized mass loss for Cs and Sr (without allowance for the shape factor of 3) versus time for UOX60 fuel subjected to external gamma irradiation (650 Gy h^{-1}) in aerated medium.

of Ar + 4%H_2, together with a decrease in the concentrations of oxidizing species; this corroborates the hypothesis that the fission products Cs and Sr are good fuel matrix alteration tracers. A major contribution by

Table 10
Results of leaching experiment 4: actinide release

Ar/H_2 (4%)	[U] (μg/L)	[U] (mol/L)	NL(U) (mg/m^2)	[^{238}Pu] (Bq/mL)	[^{238}Pu] (mol/L)	NL(^{238}Pu) (mg/m^2)	R(^{238}Pu/U)	[^{239}Pu] (Bq/mL)	[^{239}Pu] (mol/L)	NL(^{239}Pu) (mg/m^2)	R(^{239}Pu/U)
0	<0.2										
1 h	0.3	1.23E−09	0.40	<2				<2			
1 day	20	8.32E−08	26	<2				<2			
3 days	32	1.33E−07	40	<2				<2			
7 days	3	1.29E−08	6	<2				<2			
10 days	6	2.49E−08	9	<2				<2			
14 days	4	1.81E−08	7	4	2.72E−11	16	2.22	<2			
14 days (acidification)	174	7.30E−07	267	55	3.62E−10	275	1.03	2.6	4.67E−09	266	1.00
14 days (rinse)	8	3.40E−08	279	3	1.91E−11	289	1.04	<2			

Ar/H_2 (4%)	[^{240}Pu] (Bq/mL)	[^{240}Pu] (mol/L)	NL(^{240}Pu) (mg/m^2)	R(^{240}Pu/U)	[^{241}Am] (Bq/mL)	[^{241}Am] (mol/L)	NL(^{241}Am) (mg/m^2)	R(^{241} Am/U)	[^{244}Cm] (Bq/mL)	[^{244}Cm] (mol/L)	NL(^{244}Cm) (mg/m^2)	R(^{244}Cm/U)
0												
1 h	<2				<QL				<2			
1 day	<2				<QL				<2			
3 days	<2				<QL				<2			
7 days	<2				<QL				<2			
10 days	<2				<QL				<2			
14 days	<2				<QL				<2			
14 days (acidification)	5.0	2.49E−09	266	1.00	<QL				82	1.12E−10	467	1.75
14 days (rinse)	<2				<QL				5.3	7.25E−12	497	1.78

Table 11
Results of leaching experiment 4: fission product release

Ar/H_2 (4%)	$[^{137}Cs]$ (Bq/mL)	$[^{137}Cs]$ (mol/L)	$NL(^{137}Cs)$ (mg/m^2)	$R(^{137}Cs/U)$	$[^{134}Cs]$ (Bq/mL)	$[^{134}Cs]$ (mol/L)	$NL(^{134}Cs)$ (mg/m^2)	$R(^{134}Cs/U)$	[Sr] (μg/L)	[Sr] (mol/L)	NL(Sr) (mg/m^2)	R(Sr/U)
0												
1 h	209	4.75E−10	55	142	<10				1.2	1.35E−08	1280	3277
1 day	631	1.43E−09	163	6	<10				0.9	1.01E−08	971	38
3 days	3230	7.34E−09	809	20	61	9.72E−12	975	24	1.2	1.35E−08	1271	32
7 days	3980	9.04E−09	990	178	64	1.02E−11	1023	183	1.5	1.68E−08	1563	280
10 days	4680	1.06E−08	1156	129	87	1.38E−11	1364	152	1.4	1.57E−08	1468	163
14 days	4980	1.13E−08	1225	173	70	1.11E−11	1109	156	1.7	1.91E−08	1746	246
14 days (acidification)	3920	8.91E−09	1364	5	<10				1.6	1.80E−08	2233	8
14 days (rinse)	55	1.25E−10	1381	5	<10				<1			

the labile inventory would not decrease the fission product release according to the nature of the cover gas.

3.2.3. H_2O_2 production under gamma irradiation: experiments 3 and 4

The H_2O_2 concentration measured in the spent fuel leachate during experiment 3 under steady-state conditions was the same as for experiment 1, i.e. 1.2×10^{-4} mol L^{-1} (Fig. 12). The presence of chemical elements other than uranium and plutonium arising from fuel alteration thus does not modify the production of stable molecular species. It should also be noted that the fuel $\alpha\beta\gamma$ radiation field does not modify the steady-state conditions observed with the source in aerated media.

In experiment 4, a hydrogen peroxide concentration of 2×10^{-7} mol L^{-1} (Table 12) was measured by chemiluminescence after 14 days of irradiation. This is significantly higher than for doped UO_2 pellets under similar experimental conditions (experiment 2), for which the value was 3.5×10^{-8} mol L^{-1}. The cover gas thus also appears to have a significant effect on the H_2O_2 concentrations with spent fuel, but the spent fuel radiation field cannot be completely disregarded in $Ar + 4\%H_2$ compared with the quantity of H_2O_2 produced in the homogeneous solution by the gamma source.

3.3. Discussion: combined effects of α, β, γ irradiation on fuel matrix alteration

The results obtained in the presence of the gamma source are of interest from the standpoint of the impact of the α, β, γ self-irradiation fields on matrix dissolution.

Table 12 summarizes the experimental results obtained in this study, together with some published data on the effects of alpha radiolysis alone [4]. While it is clearly possible to compare the actinide release and the hydrogen peroxide concentrations in solution for the different experiments, the lack of an alteration tracer for the doped UO_2 experiments makes it difficult to

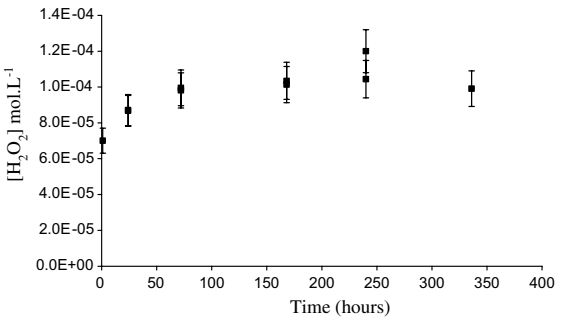

Fig. 12. Hydrogen peroxide concentration in the homogeneous solution versus time in aerated medium (experiment 3 with UOX60).

Table 12
Summary of experimental results

Doped UO_2 (1500-year batch)	Air	Ar [4]	Experiment 1: Air + external γ irradiation	Experiment 2: Ar + 4%H_2 + external γ irradiation
$R_L(U)$ (mg m^{-2} d^{-1})	0.5	0.2	83	6
$[H_2O_2]$ (mol L^{-1})	nd	$<2\times10^{-8}$	1.2×10^{-4}	3×10^{-8}

UOX 60	Air	Experiment 3: Air + external γ irradiation	Experiment 4: Ar + 4%H_2 + external γ irradiation
$R_L(U)$ (mg m^{-2} d^{-1})	0.4 (1.2)	34 (103)	6.5 (20)
$R_L(^{134}Cs)$ (mg m^{-2} d^{-1})	nd	312 (935)	27 (80)
$R_L(Sr)$ (mg m^{-2} d^{-1})	nd	295 (885)	<40 (120)
$[H_2O_2]$ (mol L^{-1})	$< 4\times10^{-6}$	1.2×10^{-4}	2×10^{-7}

() without shape factor.

Table 13
Dose rates (Gy h^{-1}) on the UOX60 fuel and α-doped surfaces under external irradiation

Irradiation	UOX60	α-doped UO_2 (1500-year batch)
α (40 μm)	1600	110
β (300–400 μm)	2300	
γ (entire water volume)	650 (+≈10)	650

determine a dissolution rate because of precipitation on the pellet surface.

Table 13 indicates the α, β, γ dose rates generated by the fuel fragments and the α dose rate corresponding to the doped UO_2 pellets. The dose rates were calculated according to the method proposed by Sunder [31] based on the α, β, γ thermal power of the fuel and the ratio of the specific stopping power values in water and in UO_2:

$$\frac{\dot{D}(H_2O)}{\dot{D}(UO_2)} = \frac{\left[\frac{1}{\rho}\frac{dE}{dx}\right]_{H_2O}}{\left[\frac{1}{\rho}\frac{dE}{dx}\right]_{UO_2}},$$

where $\dot{D}$ = dose rate (Gy h^{-1}), ρ = density (g cm^{-3}) and dE/dx = linear energy transfer (LET) (MeV cm^{-1}), which depends on the type of radiation and on the energy [31]. It is wise not to overlook the limitations of this type of calculation, which neglects some factors including: the probability of release of emitters from the matrix according to the distance between the disintegration site and the UO_2/water interface; attenuation of emitters in the UO_2 matrix before they reach the water; energy deposition profiles along the path, etc. Nevertheless, more detailed calculations [32] show that the mean α and β dose rates calculated using Sunder's method [31] are correctly estimated within a factor of 2 or 3 in the test geometries (UO_2 pellets and millimeter-size spent fuel fragments).

3.3.1. Effect of alpha self-irradiation

The effect of alpha self-irradiation on uranium release from UO_2 pellets and spent fuel fragments is masked under aerated conditions in the presence of a gamma source since both materials exhibit the same leaching behavior (Table 12) whereas the alpha dose rates at the interfaces are significantly different (110 and 1600 Gy h^{-1}). This result is consistent with the available data on leaching of doped UO_2 batches for which the alteration rate due to alpha radiolysis alone did not exceed 2 or 3 mg m^{-2} d^{-1} for the batches doped with the highest ^{238}Pu specific activity (4.75×10^8 Bq/g_{UO_2}, 15-year batch) [4]. In these experiments the uranium concentrations for this batch increased continuously over time, indicating possible kinetic control [4]. The hydrogen peroxide concentrations were also identical (1.2×10^{-4} mol L^{-1}) for experiments 1 and 3; the significant production of oxidizing species resulted mainly from external gamma irradiation.

For the experiments carried out with a gamma source in Ar + 4%H_2, the uranium release rate determined for UOX60 fuel ranged from 6.5 to 20 mg m^{-2} d^{-1} (Table 12). This rate based on uranium, which underestimates the alteration by a factor of 4 or 5, is also higher than the results (2 or 3 mg m^{-2} d^{-1}) for the batches doped with the highest ^{238}Pu specific activity (4.75×10^8 Bq/g_{UO_2} compared with 6×10^8 Bq/g_{UO_2} for spent fuel) [4]. Alpha irradiation thus also appears to have less effect on spent UOX60 fuel than beta gamma irradiation in Ar + 4%H_2 atmosphere.

3.3.2. Effect of beta self-irradiation

Only spent fuel fragments generate a beta self-irradiation field. The beta dose rate in a layer of water 300–400 μm deep on the fuel surface was estimated using Sunder's method [31] as 2300 Gy h^{-1}. The beta dose rate was thus considerably higher (by a factor of 3.5) than the gamma dose rate generated by the cobalt source.

The results obtained for actinides with the source in aerated media showed no significant difference between spent fuel and doped UO_2 pellets (experiments 1 and 3). This is also the case for H_2O_2 production. This result suggests that the spent fuel beta radiation field has no significant effect under these experimental conditions. The diffusion of oxidizing species from the bulk to the surface predominates with external gamma irradiation in aerated media.

In experiment 4, conducted in Ar + 4%H_2 with an external irradiation source, the actinide release rates were slightly higher than determined for doped UO_2 pellets (experiment 2). The H_2O_2 concentration also increased between experiment 2 and experiment 4, indicating that the fuel $\beta\gamma$ self-irradiation field can no longer be disregarded in the presence of a source in Ar + 4%H_2.

The reference experiment on spent fuel in aerated water without external gamma irradiation shows the slight impact of self-irradiation on dissolution: the mean uranium release rate was 0.4 mg m^2 d^{-1} (1.2 mg m^{-2} d^{-1} disregarding the shape factor) after 14 days (Table 3). This value is in agreement with the results reported by Forsyth [30] and Gray [33] for spent fuel fragments. The species generated by beta irradiation of the fuel thus interact very little with the surface under aerated conditions without external gamma irradiation. The dominant process in this case appears to be the diffusion of species from the surface into the homogeneous solution.

3.3.3. Effect of gamma self-irradiation

Only spent fuel fragments also have a gamma self-irradiation field; considering the fuel mass (m = 1.0147 g) in the leaching vessel and the corresponding gamma thermal power (5.48×10^2 W t_{HM}^{-1}), it is negligible (about 10 Gy h^{-1}) compared with the dose rate generated by the external gamma source. No contribution is thus expected from gamma self-irradiation of the fuel.

4. Conclusions

External gamma irradiation experiments on UO_2 pellets doped with alpha emitters and on spent fuel allowed us to assess the effects of water radiolysis on oxidizing dissolution of the fuel matrix. In particular, the experiments provided data on the effect of each type of radiation on fuel alteration; although alpha radiation will predominate over the long term, the material available for study today includes α, β, γ radiation sources. The impact of the cover gas is another significant aspect of the difficulty in view of the problems that can occur in interim storage and after geological disposal of the fuel (burst rod in a cooling pool, canister failure, groundwater ingress after 10 000 years, etc).

The following main conclusions can be drawn from the 'model' experiments on doped UO_2 pellets:

- Despite linear actinide release over time after rinsing the experimental setup with acid, the uranium and plutonium dissolution rates cannot be used to obtain the matrix alteration rates under gamma irradiation. The latter are significantly underestimated (probably by a factor of 5–10) considering the precipitation that occurs on the pellet surface. Future experiments on UO_2 pellets doped with actinides and strontium (alteration tracer) will provide an accurate determination of these alteration rates.
- The nature of the cover gas has a major effect on the mechanism of oxidizing dissolution of the UO_2 matrix in an external gamma irradiation field of 650 Gy h^{-1}. The uranium dissolution rate in an aerated medium is 83 mg m^{-2} d^{-1} compared with only 6 mg m^{-2} d^{-1} in Ar + 4%H_2. The rate drop is accompanied by a reduction of about four orders of magnitude in the hydrogen peroxide concentrations in the homogeneous solution.
- Although they underestimate the actual alteration, the rates based on the actinide release nevertheless show that the contribution of alpha radiolysis generated by a lightly doped pellet (0.7×10^8 Bq/g_{UO_2}, 1500-year batch) is negligible compared with the gamma source in aerated media.
- In Ar + 4%H_2 the effect of gamma radiolysis generated by an external source (650 Gy h^{-1}) remains greater than the effect of alpha radiolysis generated by a lightly doped pellet (0.7×10^8 Bq/g_{UO_2}, 1500-year batch).

The experiments with spent fuel fragments produced the following results:

- The fission products Cs and Sr constitute good spent fuel matrix alteration tracers, considering the preleaching history and congruence observed between strontium and cesium during leach tests under gamma irradiation. The tracers demonstrate that 80–90% of the actinides precipitate on the surface of the spent fuel fragments, depending on the experimental conditions.
- The spent fuel alteration rate is highly dependent on the nature of the cover gas, as is the production of oxidizing species. The alteration rate drops by an order of magnitude in Ar + 4%H_2 compared with air, and the hydrogen peroxide concentration drops by three orders of magnitude.
- The greater the hydrogen peroxide concentration, the higher the alteration rate. The radicals appear to have a major role under external gamma irradiation, however, in view of the rates obtained, which exceed the values observed in the reference experiments (H_2O_2 added without external gamma irradiation).

- The dissolution rates of actinides from spent fuel and doped UO_2 pellets, and the quantities of oxidizing species (H_2O_2) determined under gamma irradiation in aerated media were identical. The fuel chemistry had no appreciable effect on alteration under these conditions.
- In Ar + 4%H_2, the fuel $\beta\gamma$ self-irradiation field cannot be disregarded since the H_2O_2 production is significantly higher than with doped UO_2.

The promising experimental approach adopted here will be pursued to quantify the influence of several parameters on the UO_2 matrix alteration kinetics including: the possible inhibiting effect of the hydrogen concentration in solution, the nature of the redox conditions (iron additive) or the nature of the radicals (using a cobalt source that modifies the nature of the cover gas). Work is now in progress to model the radiolysis phenomena at the interfaces.

Acknowledgement

Financial support for this research has been provided in the framework of the CEA-PRECCI program (C. Poinssot and C. Ferryas part of CEA-EDF (J.M. Gras) agreement. The experimental data were obtained in the *Atalante* facility and the work of M. Bonnal, C. Marques, B. Charles, M. Desir and A. Gavazzi in the hot cell laboratory is gratefully acknowledged. The authors are grateful to the referee whose remarks allowed significant improvements in the presentation and interpretation of their results.

References

[1] D.W. Shoesmith, S. Sunder, J. Nucl. Mater. 190 (1992) 20.
[2] D.W. Shoesmith, J. Nucl. Mater. 282 (2000) 1.
[3] C. Poinssot, C. Jégou, P. Toulhoat, J.-P. Piron, J.-M. Gras, Mat. Res. Soc. Symp. Proc. 663 (2000).
[4] C. Jégou, V. Broudic, A. Poulesquen, J.M. Bart, Mat. Res. Soc. Symp. Proc. 807 (2004).
[5] V.V. Rondinella, Hj. Matzke, J. Cobos, T. Wiss, Radiochim. Acta. 88 (2000) 527.
[6] J. Cobos, L. Havela, V.V. Rondinella, J. De Pablo, T. Gouder, J.P. Glatz, P. Carbol, H. Matzke, Radiochim. Acta. 90 (2002) 1.
[7] W.J. Gray, Effect of surface oxidation, alpha radiolysis, and salt brine composition on spent fuel and uranium dioxide leaching performance: Salt Repository Project, Pac. Northwest Lab., Richland, WA, USA, Report PN_L/SRP-6689, 1988.
[8] J.P. Grouiller, J. Pavageau, In synthesis on the spent nuclear fuel evolution, CEA R-5958 report (ISSN04293460), 2001, 616 p.
[9] C. Jégou, S. Peuget, V. Broudic, D. Roudil, X. Deschanels, J.M. Bart, J. Nucl. Mater. 326 (2004) 144.
[10] Hj. Matzke, J. Nucl. Mater. 189 (1992) 141.
[11] J.W. Spinks, R.J. Woods, An Introduction to Radiation Chemistry, 3rd Ed., Wiley–Interscience, New York, 1980.
[12] Hochanadel, J. Phys. Chem. 56 (1952) 587.
[13] V. Trupin-Wasselin, Processus primaires en chimie sous rayonnement. Influence du Transfert d'Énergie Linéique sur la radiolyse de l'eau, PhD thesis, University of Paris-Sud-Orsay, France, 2000.
[14] V. Broudic, B. Muzeau, C. Jégou, M. Bonnal, A. Gavazzi, C. Marques, in: International Conference Atalante 2004, 21–24 June 2004, Nîmes, France, p. 2.
[15] A. Loida, B. Grambow, H. Geckeis, J. Nucl. Mater. 238 (1996) 11.
[16] R.S. Forsyth, The SKB Spent Fuel Corrosion Program, SKB Technical Report 97-25, December 1997.
[17] H. Christensen, S. Sunder, Nucl. Technol. 131 (2000) 102.
[18] A.O. Allen, The Radiation Chemistry of Water and Aqueous Solutions, D. Van Nostrand, Princeton, 1961.
[19] P. Kirkegaard, E. Bjergbakke, CHEMSIMUL, a program package for numerical simulation of chemical reaction systems, Riso National Laboratory DK-4000 Roskilde Denmark, 20 November 1998.
[20] H. Christensen, S. Sunder, J. Nucl. Mater. 238 (1996) 70.
[21] H. Christensen, S. Sunder, D.W. Shoesmith, J. Alloys Comp. 213/214 (1994) 93.
[22] H. Christensen, Nucl. Technol. 124 (1998) 165.
[23] G. Sattonnay, C. Ardois, C. Corbel, J.F. Lucchini, M.F. Barthe, F. Garrido, D. Gosset, J. Nucl. Mater. 288 (2001) 11.
[24] W.J. Gray, G.L. McVay, Radiat. Eff. 89 (1985) 257.
[25] H. Karasawa, E. Ibe, S. Uchida, Y. Etoh, T. Yasuda, Radiat. Phys. Chem. 37 (1991) 193.
[26] M. Amme, Radiochim. Acta 90 (2002) 399.
[27] J. Van Der Lee, L. De Windt, CHESS Tutorial and Cookbook, Updated for version 3.0, Users manual Nr LHM/RD/02/13, École des Mines de Paris, Fontainebleau, France, 2002.
[28] T.J. Wolery EQ3/6: A software package for geochemical modelling of aqueous systems: package overview and installation guide (version 7.0) (UCRL-MA-110662 PT I ed.), Lawrence Livermore National Laboratory, 1992.
[29] P. Vitorge, H. Capdevilla, S. Maillard, M.H. Faure, T. Vercouter, J. Nucl. Sci. Technol. (Suppl. 3) (2002) P713.
[30] R.S. Forsyth, L.O. Werme, J. Nucl. Mater. 190 (1992) 3.
[31] S. Sunder, Nucl. Technol. 122 (1998) 211.
[32] C. Jégou, A. Poulesquen, Calculation of alpha radiation dose rate in a water layer in contact with UO_2 grain, personal communication.
[33] W.J. Gray, D.M. Strachan, Mater. Res. Soc. Symp. Proc. 212 (1991).